Effect of mode cut-off on dispersion in photonic bandgap fibers

J. Jasapara, R. Bise, T. Her, and J. W. Nicholson

OFS Laboratories,
600 Mountain Ave.,
Murray Hill, NJ 07974.
Ph.: (908) 582-3234, email: jasapara@ofsoptics.com

Abstract: The phase dispersion of the fundamental mode in two different photonic bandgap fibers is measured and compared. The difference in dispersion behavior is attributed to the location of the mode cut-off relative to the bandgap.

OCIS codes: (060.2270) Fiber characterization; (260.2030) Dispersion

In a photonic bandgap (PBG) fiber confinement of light to the core occurs through reflections off the 2-D periodic microstructure surrounding the core. This unique confinement mechanism, as opposed to total internal reflection guidance in conventional optical fibers, gives rise to interesting dispersion properties in PBG fibers that are strongly influenced by the crystal structure [1, 2]. Transmission applications require a low and flat dispersion, whereas dispersion compensation or other device applications may require high dispersions. The advantage of bandgap fibers is that depending upon the application, the crystal structure can be designed to achieve the required dispersion profile. We have measured the dispersion of two different PBG fibers (called fibers A and B respectively) using spectral interferometry with supercontinua. Fiber A is multi-moded across the bandgaps whereas fiber B is single-moded. In this paper we show that the dispersion is strongly affected by where the mode-cutoff of the fiber occurs relative to the bandgap.

Fibers A and B have a triangular lattice of air holes surrounding a solid silica core. The holes are filled with a high index liquid which raises the average index of the cladding to above that of the core, thereby enabling guidance via the bandgap effect as opposed to the index guidance mechanism. Figure 1 shows the transmission spectrum of the two fibers.

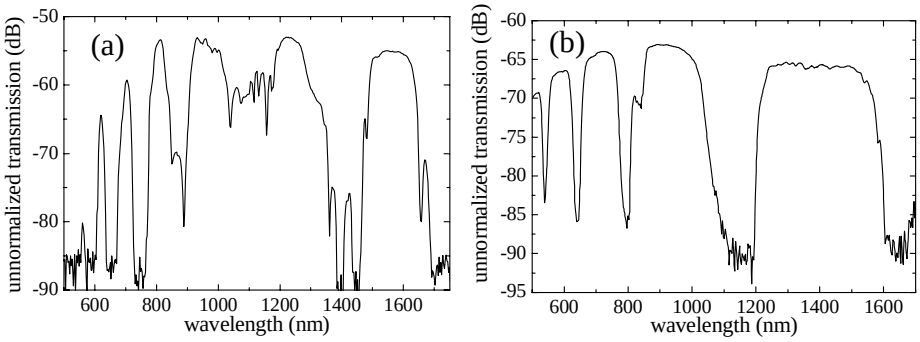

Fig. 1. Transmission spectrum of (a) fiber A, and (b) fiber B. Hole spacing $\Lambda = 4.3$ μm, hole diameter $d = 2.3$ μm, and index of holes $n_d = 1.8$ for fiber A. $\Lambda = 5.5$ μm, $d = 2.2$ μm, and $n_d = 1.59$ for fiber B.

Spectrally resolved near-field modes of the fibers were recorded. Super-continuum generated in nonlinear fibers was spectrally filtered to bandwidths < 2 nm with a monochromator and sent through the PBG fibers. The output of the fibers was imaged. The insets of Fig. 2 show the modes across the bandgaps of fibers A and B. For all bandgaps of fiber A the fundamental mode dominates on the short wavelength side of the bandgap spectrums. The fundamental mode is abruptly cutoff within 5 nm of the transmission peak as the wavelength increases and beyond the mode cutoff only the higher order mode is supported. In fiber B the fundamental mode extends across the entire bandgap (for all bandgaps) and it was impossible to excite higher order modes by skewing the launch conditions. Hence fiber A is multi-moded while fiber B is single-moded.

The dispersion of the fundamental mode of the fibers was measured with spectral interferometry using supercontinuum generated in highly nonlinear fibers for measurements across different transmission windows (see Refs. [1,2] for details). The dispersion of Fiber A was measured for bandgaps lying in the visible using a

supercontinuum generated in a high delta microstructured fiber [3] and is shown in Fig. 2(a). Dispersion of Fiber B was measured over a single bandgap that spanned from ~ 1200 nm to ~ 1600 nm using continuum generated in a dispersion managed span of highly nonlinear fiber [4] and is shown in Fig. 2(b). The measured dispersions for both fibers exhibit an inflection point as they go from negative values at short wavelengths to positive values at long wavelengths and are both asymmetric with larger dispersion (relative to the inflection point) at the long wavelength edge than at the short wavelength edge. The inflection is reminiscent of the dispersion due to reflection off a periodic resonant structure. However the dispersion of fiber A is an order of magnitude higher and more asymmetric relative to the inflection point, than fiber B near the long wavelength edge of the bandgap. In addition the inflection point in the dispersion of B is shifted to positive values compared to A because the material dispersion is positive at infra-red wavelengths and negative at visible wavelengths.

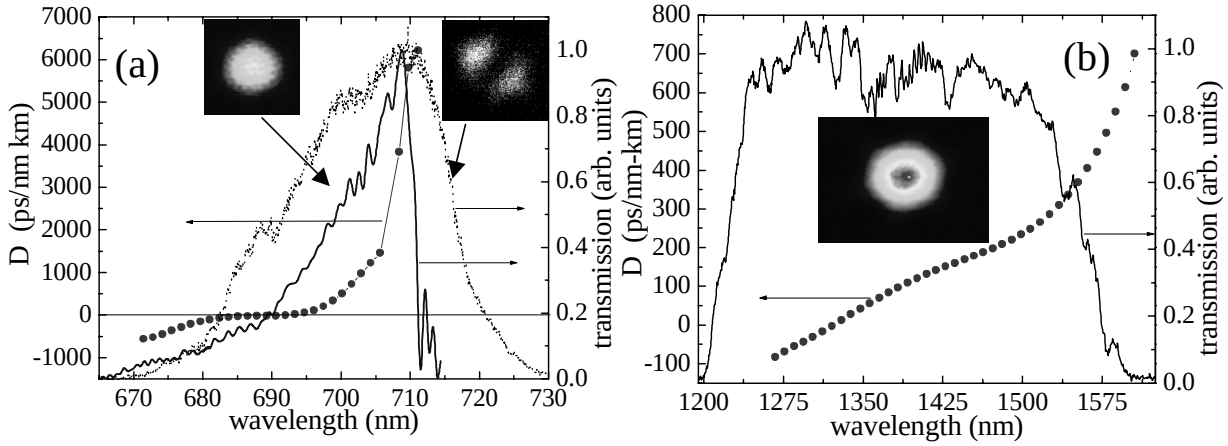

Fig. 2. Phase dispersion (dotted curve) and transmission (solid and dashed curves) measured across bandgaps of fiber A (a), and fiber B (b). In (a) the solid line is the transmission of the fundamental mode only measured in the spectral interferometry setup. The dashed line is the total transmission in all modes. The insets show the measured spectrally resolved near-field mode images of the fibers.

The main features of the dispersion can be explained qualitatively by a 2-D model waveguide (see Fig. 3(a)) consisting of a core region surrounded by a stack of thin films which act as scattering centers [2]. When a

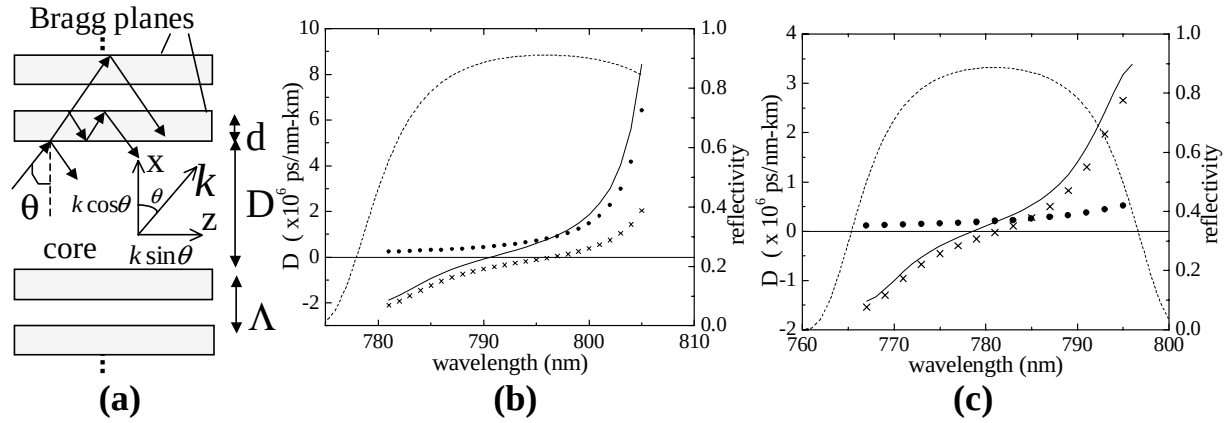

Fig. 3. (a): Geometry of propagation in a 2-D waveguide surrounded by a stack of thin films. For the calculations a stack of 10 films of thickness 2.4 μm, index 1.78, imbedded in silica of index 1.45 and separated by 4.3 μm was assumed. (b) and (c): Contribution of the various components to the dispersion for the case where the mode cutoff is at 808 nm (b) and 811 nm (c). The dotted curve is the contribution of the longitudinal component, the curve with crosses is the contribution due to reflection, and the solid line is the total dispersion. The dashed lines are the reflectivity of the film stack under the condition that the transverse component is held a constant. P-polarized light was assumed for the calculations.

wavefront propagates a longitudinal distance $L = D\tan(\theta)$, the phase change seen by it is given by (see Fig.

3(a)),

$$\Phi(\omega,\theta) = Lk\sin[\theta(\omega)] + Dk\cos[\theta(\omega)] + \phi_r(\omega), \tag{1}$$

where ϕ_r is the phase change on reflection off the periodic strucuture, $k = 2\pi c/\lambda$ is the wave vector, c is the speed of light, λ is the free space wavelength, and $\omega = ck$ is the angular frequency. Guidance by the bandgap effect requires that for all wavelengths the transverse component satisfy the Bragg condition for reflection, i.e. $k\cos[\theta(\omega)] = 2\pi m/\Lambda = \text{constant}$, where m is an integer. This implies that (a) the transverse component does not contribute to the dispersion, and (b) the angle of propagation is a function of the wavelength, $\theta(\lambda) = \cos^{-1}(m\lambda/\Lambda)$. Hence the dispersion due to propagation is,

$$\frac{d^2\Phi}{d\omega^2} = L\frac{d^2k\sin[\theta(\omega)]}{d\omega^2} + \frac{d^2\phi_r}{d\omega^2}. \tag{2}$$

Figures 3 (b) and (c) show the contribution of the two terms to the dispersion calculated under the condition that the transverse wave vector is held constant. The wavelength at which the transverse wave vector component can no longer satisfy the Bragg condition ($k > 2\pi m/\Lambda$), defines the mode cutoff. For Fig. 3 (b) the mode cut-off was chosen to lie within the bandgap and for Fig. 3 (c) the mode cutoff was chosen to lie outside the bandgap. The reflection from the periodic crystal structure surrounding the core (second term in Eqn. 2) gives rise to the inflection in the dispersion curves and this is the signature of a resonant structure. The imposition of the Bragg condition on the transverse component of the wave vector increases the group delay with increase in wavelength leading to a fast rising component to the dispersion at the long wavelength edge (first term in Eqn. 2). We see that in the case of Fig. 3 (b) the dispersion increases very rapidly near the edge of the bandgap and this makes the curve highly asymmetric, whereas in the case of Fig. 3 (c) the increase at the edge of the bandgap is gentler and the dispersion is more symmetric relative to the inflection point. Hence where the mode cutoff occurs relative to the reflection band of the Bragg structure defines the strength of dispersion of the longitudinal wave vector component and hence the sharpness of the increase at long wavelengths.

These studies give a valuable insight into the physical mechanisms that affect the phase response of light propagating in the bandgaps. This knowledge can be used to tailor the dispersion of bandgap fibers to suit the application. For example, if a flat dispersion profile is desired over the bandgap, the crystal structure must be designed so that the mode cutoff does not overlap with its reflection bands. On the other hand if large positive dispersion values are required, the crystal structure must be designed so that the mode cut off lies within its reflection band.

References

1. J. Jasapara, R. Bise, and R. Windeler, *Optical Fiber Communication* (Anaheim, CA, 2002), pp. 519–521.
2. J. Jasapara, *Symposium on Optical Fiber Measurements* (Boulder, CO, 2002).
3. J. K. Ranka, R. S. Windeler, and A. J. Stentz, "Visible Continuum Generation in Air-Silica Microstructure Optical Fibers with Anomalous Dispersion at 800 nm," Optics Letters **25,** 25–27 (2000).
4. J. Nicholson, M. Yan, A. Yablon, P. Wisk, J. Fleming, F. DiMarcello, and E. Monberg, "A high coherence supercontinuum source at 1550 nm," submitted to OFC (2002).